

Interplanetary disturbances and their association with large-scale magnetic field on the sun

P.K. Manoharan

Radio Astronomy Centre (NCRA), Tata Institute of Fundamental Research, Udthagamandalam (Ooty) 643 001, India

Abstract. The principal purpose of this paper is to review recent progress in the study of three-dimensional aspects of interplanetary disturbances on the basis of interplanetary scintillation measurements. The scintillation technique exploits the scattering of radio waves from distant cosmic sources by the density turbulence in the solar wind and interplanetary disturbances are identified by the increase in the level of density turbulence compared with the ambient solar wind. In the present study, scintillation observations obtained within 1 AU using the Ooty Radio Telescope have been analyzed to study a large number of disturbances between minimum (August 1986) and maximum (April 1991) of the previous solar cycle. The spatial and dynamical distribution of these disturbances are compared with results from the Solar Maximum Mission (SMM) K-corona data and other solar measurements. The results indicate that most of the disturbances are associated with active prominences on the sun, which are suggested to be the source of coronal mass ejections (CMEs).

Key words: sun: activity - flare -coronal mass ejection; interplanetary medium: solar wind - disturbance

1. Interplanetary disturbances

The sun produces a variety of energetic and eruptive phenomena such as solar flares, eruptive prominences, coronal mass ejections, high-energy particles and the continuous flow of solar wind, which add great concentration of plasma, energy and magnetic field to the solar wind. A major solar-wind disturbance (or transient) that propagates out through interplanetary space, depending on a variety of interplanetary configurations, may affect the earth and its magnetosphere. The disturbances in the solar wind are classified as sporadic or recurrent. The latter are causally associated with coronal holes on the sun and are typically observed near the ecliptic plane at distances ≥ 1 AU. The sporadic, non-recurrent transients in the solar wind are caused by the injection of mass from the sun into interplanetary space. The history of solar-terrestrial studies, starting from Carrington (1860), has shown a clear, although far

from perfect, correlation between flares and geomagnetic storms. However, the growing observational evidences, acquired since the beginning of the space age in 1960s, have raised many questions concerning the connection of interplanetary disturbances with solar flares (Gosling 1993 and references therein). Nowadays, many investigators believe that travelling interplanetary disturbances, large solar energetic events and major non-recurrent geomagnetic storms are produced by coronal mass ejections, CMEs (Reames 1995). There are several observational methods to study such coronal disturbances in the near-sun region and also close to the earth's orbit. The study of cause and effect in energetic transients, however, requires good spatial and temporal coverage in the large observational gap between the sun and earth. The interplanetary scintillation technique is applicable for the dedicated remote sensing of interplanetary space in the distance range 20-200 solar radii (R_{\odot}). The purpose of this paper is to review the properties of the interplanetary disturbance, particularly within 1 AU of the sun, based on scintillations data obtained with the Ooty Radio Telescope (Swarup et al. 1971).

2. Estimations of density turbulence and velocity

The interplanetary scintillations (IPS) arise when the radio waves from a distant compact source are scattered by small-scale (10-1000 km) density irregularities in the solar-wind plasma (Hewish et al. 1964). In order to compare IPS from various sources on different days, the normalized scintillation index, g , of a given source is determined by normalizing the measured level of scintillation using the average "scintillation-distance (ΔS -R)" curve of the same source, i.e., $g = \frac{\Delta S(R)}{\langle \Delta S(R) \rangle}$. The g -value remains close to unity when the solar wind flow is undisturbed, whereas $g > 1$ represents the presence of a transient in the solar wind. Figure 1a gives an example of a disturbance corresponding to the solar event on 29 September 1989 at S26°W90°. The level of scintillation, in the quasi-static solar wind condition, is heavily weighted to the plasma characteristics in the region of closest approach of the line of sight to the sun. But, when a transient crosses the line of sight at position other than the closest point of approach, the estimated locations of the disturbance in the heliosphere and on the solar surface (discussed in the later section) may have positional uncertainty. The positional error, however, is always less than 30° in heliographic coordinates (Manoharan 1997).

The primary interest of the transient's study is to trace the interplanetary disturbances back to the solar surface with the help of their speed information, so that they may be compared with coronal features. The possibility of measuring the solar-wind velocity using the single-antenna system (Manoharan & Ananthakrishnan 1990; Manoharan 1995) provides an excellent opportunity to obtain the velocity coverage of the interplanetary medium. In this method, the speed is determined from the power spectrum of scintillation with a reasonable assumption for the turbulence spectrum. However, the estimation of speed and the normalization of scintillation are valid only in the weak-scintillation regime, which occurs at distances greater than 40 R_{\odot} for 327 MHz measurements (Manoharan 1993).

Routine IPS measurements are being made at Ooty over many years, which also include many solar wind disturbances. The observational details and analysis procedure are given by Manoharan (1997). In brief, the main points, relevant for the data discussed in this paper, are: (i) measurements presented here cover a period August 1986 to April 1991, (ii) Nearly

15 sources have been observed per day over 6-8 hr daylight period, (iii) disturbances are selected by the criterion that the observed g values are greater than 1.4, and (iv) in total, 738 scintillation enhancements (or disturbances) are identified. The simultaneous estimation of both g and speed, as demonstrated by Manoharan et al. (1995), contributes to our understanding of the solar manifestation and the related travelling interplanetary disturbance.

3. Spatial and kinematical distributions

The frequency of occurrence of interplanetary disturbances correlates well with the 11-year sunspot cycle as shown in Fig. 1b, which indicates a factor of three higher disturbance rates in solar maximum (1991) than during minimum (1986). This is consistent with the CME observations and when the scintillation-observation timing is normalized for the full disk of sun, the number of disturbances per day, ~ 2 , is in agreement with mass ejection rate at solar maximum (Webb & Howard 1994). These results are also in agreement with transient measurements obtained from the Doppler-scintillation technique during 1979-1987 at distances inside $100 R_{\odot}$ (Woo 1993) and the survey of interplanetary disturbances made using the Pioneer Venus Orbiter (PVO) magnetometer and plasma data between 1979 and 1988 at 0.72 AU (Lindsay et al. 1994).

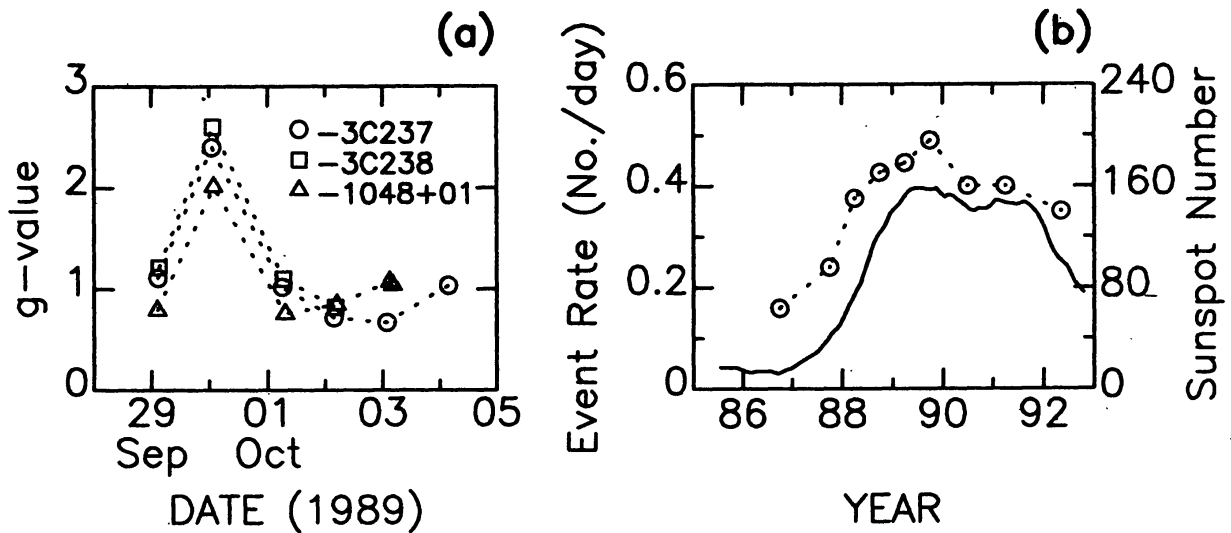


Figure 1. (a) The g values versus date plot for the interplanetary disturbances, caused by the solar event on September 29, 1989, as observed at Ooty. This disturbance was seen, nearly simultaneously, at lines of sight to many nearby ecliptic radio sources and among them, g values from three sources are plotted. (b) Comparison between sunspot number (continuous line) and interplanetary disturbance occurrence rate (dotted line, joining circles) from August 1986 through mid 1992.

Another important fact about interplanetary disturbances is the spatial distribution with significant variations over heliolatitudes, as displayed in Fig. 2a. This plot reveals the long-term variations and in particular the rapid spread of disturbances to high heliolatitudes during 1989-90, the maximum phase of the sunspot cycle. Thus, the disturbances are not always confined to the equatorial belt of the heliosphere, where solar flares normally originate. The adjacent panel in the figure is the plot of solar-flare latitudes, which includes all types of flares seen in $H\alpha$ (Solar-Geophysical Data Reports, U.S. Department of Commerce). It is

interesting to note that these flare latitudes slowly drift towards the solar equator during solar maximum, whereas the disturbance latitudes spread to higher latitudes. The behaviour of changing spatial location of disturbances is similar to the distribution of CMEs observed with the Solar Maximum Mission (SMM) between 1980 and 1989 (Hundhausen 1993).

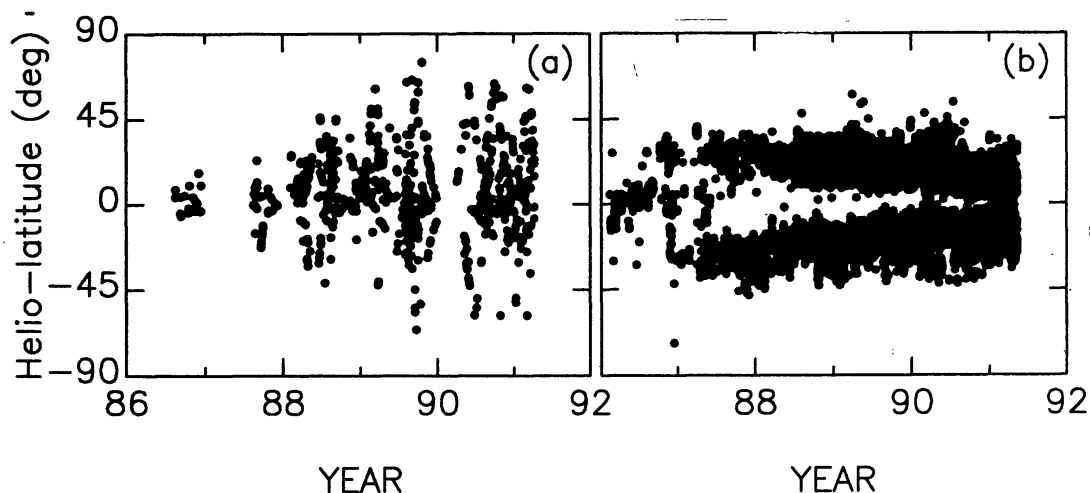


Figure 2. (a) The latitude distribution of interplanetary disturbances plotted as a function of year. Near solar minimum (1986–mid-1988), disturbances are close to the equatorial region of the sun; as activity increases, the outer envelope of the distribution rapidly spreads to higher helio-latitudes. Similar behaviour is also seen in the latitude pattern of CMEs observed with the SMM (Hundhausen 1993). (b) Latitudes of all types of solar flares observed in H α .

The kinematical description of all these disturbances is based on the single-station velocity estimation method (Manoharan & Ananthakrishnan 1990). The bias in the estimated speed, caused by the effect of projection, is small (<15%), because a large angle of projection reduces the detectability of scintillation enhancement (or $g \geq 1.4$) at any given heliocentric distance (Manoharan 1997). Fig. 3a is a histogram of speeds. A wide range of speeds is found, from $\sim 200 \text{ km s}^{-1}$ to as high as $\sim 1600 \text{ km s}^{-1}$, implying coronal transients with a variety of injection speeds into the solar wind. Nearly 80% of the speeds lie in the range $450 \pm 200 \text{ km s}^{-1}$. The range of speeds and their mean value are consistent with those for the CME velocities with an average of $\sim 450 \text{ km s}^{-1}$ observed with the SMM (Hundhausen et al. 1994). It is also interesting to note that the disturbance speed does not show any preferential latitude. That is, when the latitudinal dependence (Fig. 2a) is checked for three ranges of disturbance speed ($V \sim 400 \text{ km s}^{-1}$, $400 < V \leq 650 \text{ km s}^{-1}$ and $V > 650 \text{ km s}^{-1}$), albeit the reduced number of data points in each speed bin it is revealing that no significant change is observed in the distribution pattern. In Fig. 3b, measured g values and their corresponding speeds are plotted and no significant correlation is observed, whereas, in the case of steady-state solar wind, the speed anticorrelates with the density (or density turbulence) (e.g., Manoharan 1993 and 1995). It can be inferred from the present study that the concentration of mass in a disturbance and the throw velocity may not correlate with each other.

The main aim of the disturbance study is to identify the cause and effect in solar activity. The broad study of CMEs has confirmed the eruption of prominence (i.e., eruption of substantial amount of plasma and magnetic field from the corona) to be the most common form of

associated activity for mass ejections (e.g., St. Cyr and Webb 1991). Therefore, the disturbances are mapped back to the solar surface with the estimated speeds along the radial path and compared with the nearest active prominence location (Solar-Geophysical Data Reports, U.S. Department of Commerce) in both space and time. Figure 4a shows the histogram of separation of the nearest active prominences from the footprint positions of all the disturbances. More than 80% of the disturbances lie close to the active prominences within 20° of heliographic coordinates, which is less than half of the width of mass ejections (St. Cyr & Burkepile, 1990). A test for the statistical significance of the above histogram is carried out by shifting the footprint location by about half solar rotation and the resulting wide-spread histogram clarifies that the disturbances' association with active prominences is not by mere chance.

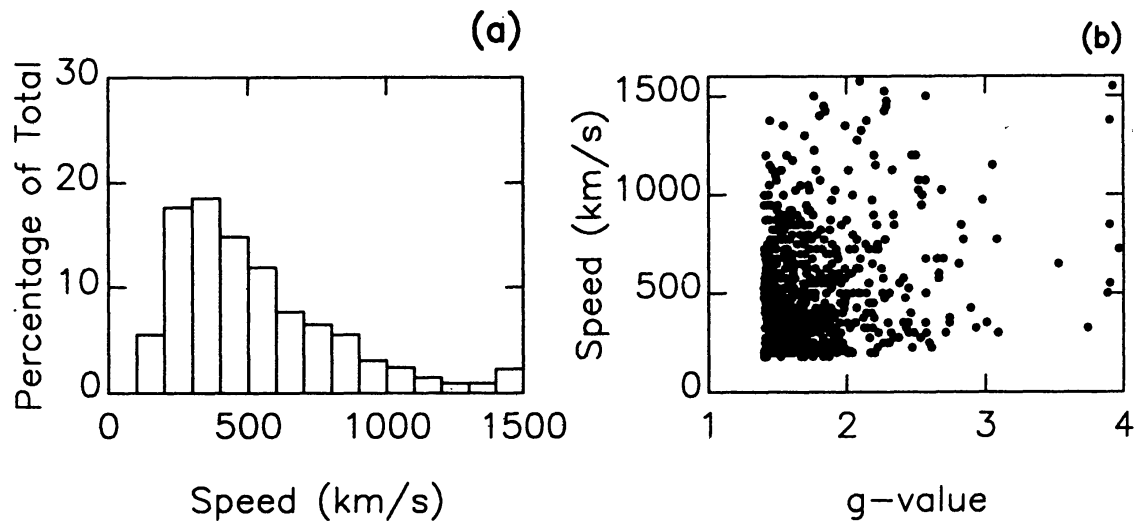


Figure 3. (a) Histogram of propagation speeds of all disturbances, shown in Fig. 2a, in intervals of 100 km s^{-1} . The last interval contains all values greater than 1500 km s^{-1} . (b) Comparison between the strength of disturbance (g value) and the propagation speed for the data presented in Figure 2a.

The latitudinal-dependence plot (Fig. 2a) shows the rarity of disturbance in the coronal-hole (or polar) regions during the minimum phase of the solar cycle, which has also been revealed by other solar wind and CME measurements (Woo & Gazis, 1993; Hundhausen 1993). However, the Cambridge group has inferred from IPS observations that CMEs arise from the coronal holes (Hewish & Bravo 1986). Therefore, the traced-back footprints on the solar surface are also compared with the nearest boundary of the coronal hole and the corresponding histogram is plotted in Figure 4b. It is evident that no clear association is observed. It should be noted that the Cambridge group measures the 81-MHz scintillation, which corresponds to heliocentric distances $>0.7 \text{ AU}$. Typically at larger distances, $\sim 1 \text{ AU}$, the formation of co-rotating interaction region (CIR) is possible. Also, in particular, the Cambridge group has observed disturbances, which predominantly appear to co-rotate with the sun (e.g. Hewish & Bravo 1986). However, the present Ooty measurements are well within 1 AU . It is also important to note that in the present study, the occurrence rate of disturbances correlates with the sunspot cycle (Fig. 2b), whereas in case of CIRs, exactly opposite trend is found (Lindsay et al. 1994).

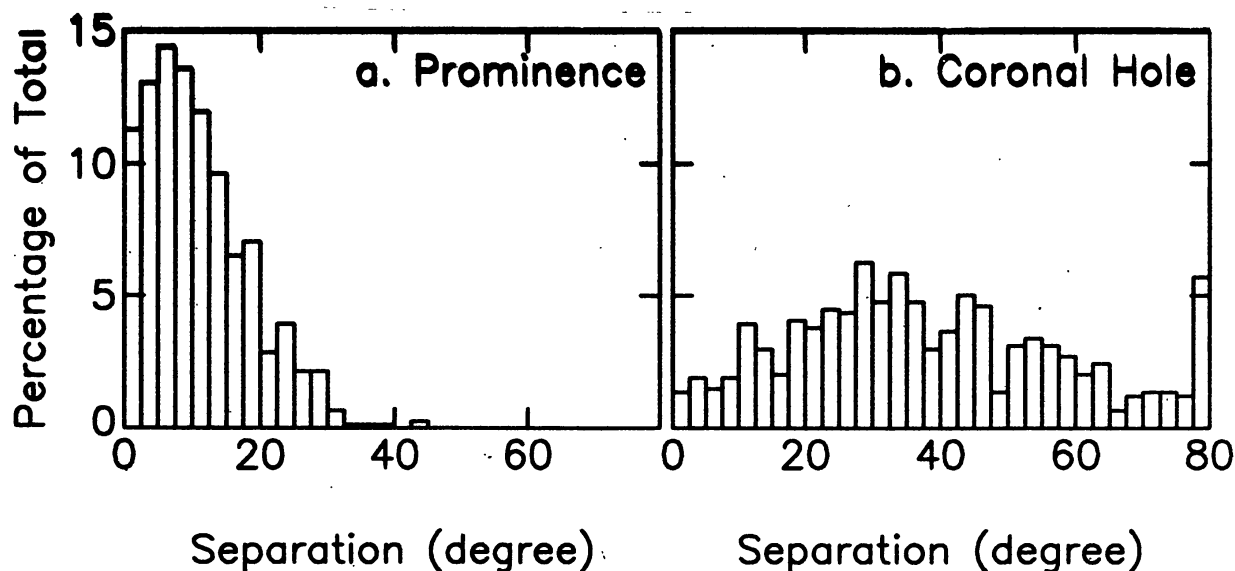


Figure 4. (a) The footprints on the sun of the interplanetary disturbances, shown in Fig. 2a, are compared with the nearest prominence in space and time. (b) The footprints of the disturbances are compared with the nearest coronal hole boundary. The last bin contains all values greater than 80° .

4. Summary

It is demonstrated in this paper that the interplanetary scintillation technique is very useful for detecting and studying interplanetary disturbances, especially in the three-dimensional inner heliosphere, where direct measurements have so far not been possible. The g value, a measure of disturbance's strength and speed can be used not only for studying the properties of the disturbance but for also forecasting the arrival time of disturbance at the earth. The present results on: (i) rate of occurrence and its correlation with sunspot cycle and frequency of CMEs, (ii) latitudinal distribution as a function of solar activity and its agreement with the distribution of CMEs, (iii) kinematical properties, and (iv) disturbance footprint's association with active prominences, agree with other transient studies and are also consistent with the statistical properties of CMEs. It is also inferred from this study that the speed and the density turbulence (or density) of disturbances are not one-to-one related. Some of these results provide convincing evidence that interplanetary disturbances are associated with active prominences and their related mass ejections. Based on these results, it is felt that measurements on individual disturbances, *at various distances* between near-sun region and earth, are crucial to infer the evolution of disturbance. Accordingly, further observations are being carried out at Ooty in collaboration with other solar observatories.

Acknowledgements

I am grateful to the observing staff of the Radio Astronomy Centre, Ooty, for help with the observations. I thank Professor V.R. Venugopal for critical reading of the manuscript.

References

- Carrington R.C., 1860, MNRAS, 20, 13.
Gosling J.T., 1993, J.Geophys. Res., 98, 18937.
Hewish A., Bravo S., 1986, Solar Phys., 106, 185.
Hewish A., Scott P.F., Wills D., 1964, Nature, 203, 1214.
Hundhausen A.J., 1993, J. Geophys. Res., 98, 13177.
Hundhausen A.J., Burkepile J.T., St. Cyr O.C., 1994, J. Geophys.Res., 99, 6543.
Lindsay G.M., Russell C.T., Luhmann J.G., 1994, J. Geophys. Res., 99, 11.
Manoharan P.K., 1993, Solar Phys., 148, 153.
Manoharan P.K., 1995, BASI., 23, 399.
Manoharan P.K., 1997, Geophys. Res. Lett., (Submitted).
Manoharan P.K., Ananthakrishnan S., 1990, MNRAS, 244, 691.
Manoharan P.K., et al., 1995, Solar Phys., 156, 377.
Reames D.V., 1995, Eos Transactions, 76, 405.
St. Cyr O.C., Burkepile J.T., 1990, A catalogue of mass ejections observed by Solar Maximum Mission Coronagraph, NCAR Technical Note NCAR/TN-352+STR, Boulder.
St. Cyr O.C., Webb D.F., 1991, Solar Phys., 136, 379.
Swarup G. et al., 1971, Nature Phys. Sci., 230, 185.
Webb D.F., Howard R.A., 1994, J. Geophys. Res., 4210.
Woo R., 1993, J. Geophys. Res., 98, 18999.
Woo R., Gazis P., 1993, Nature, 366, 543.